Available online at www.sciencedirect.com
SCIENCE DIRECT®
International Journal of Thermal Sciences 42 (2003) 639–646
International Journal of Thermal Sciences
www.elsevier.com/locate/ijts

Prediction and measurement of soot particulate formation in a confined diesel fuel spray-flame at 2.1 MPa

R.J. Crookes [a,*], G. Sivalingam [b], M.A.A. Nazha [c], H. Rajakaruna [c]

[a] *Department of Engineering, Queen Mary, University of London, Mile End Road, London E1 4NS, UK*
[b] *Ford Motor Company plc, Dunton Technical Centre, Laindon, Basildon, Essex SS15 6EE, UK*
[c] *Department of Engineering and Technology, De Montfort University, The Gateway, Leicester LE1 9BH, UK*

Received 13 May 2002; accepted 19 November 2002

Abstract

A high-pressure combustion system able to provide stable continuous combustion of a liquid fuel spray under closely controlled reproducible steady conditions at pressures approaching those of diesel engine operation is described. The system provides ready access and time for gaseous and particulate samples to be taken for analysis from the exhaust and selected locations inside the flame. Measurements provide data for comparison with available mathematical models. A relatively fast and efficient spray combustion model, including soot formation and oxidation, has been used to compare the predicted values with the results of the experimental tests at a gauge pressure of 2 MPa.

The computer programme qualitatively predicted the influence of pressure and input equivalence ratio on the formation and distribution of soot inside the combustion chamber. Increasing peak soot concentration at higher pressure and higher input equivalence ratio was measured and predicted, with off-axis maximum values in an annulus around the axial peak value. Measurements of primary-particle diameters in soot agglomerates sampled at different operating conditions and locations in the spray flame gave number-mean primary-particle diameters in the range 20 to 50 nm. Larger values were measured at the highest chamber pressures and input equivalence ratios.

Keywords: Spray-combustion; Soot particulates; Diesel fuel; High-pressure burner

1. Introduction

Soot particulate emissions from diesel engines are a major factor limiting the more widespread adoption of these engines as automotive power plant. The processes taking place in a diesel engine during combustion of a fuel spray are complex and computer models describing them need to be experimentally validated with precise data. Prediction of the exhaust smoke levels requires a knowledge of the formation and oxidation mechanisms of carbon particulates and an understanding of the effect of the governing properties on the kinetics.

Measurements of particulate matter inside the combustion chamber of a running diesel engine are difficult to make, while measurements in the exhaust need to be carefully correlated with in-cylinder events. It is necessary, therefore, for validating computer models, to have experimental data under carefully controlled steady conditions. Laboratory gas burners usually operate at conditions remote from those of diesel engines and combustion bomb, shock-tube and rapid compression machine experiments have similar spatial and temporal limitations to engine tests. Soot volume fractions may also be so high, at elevated pressures, that light obscuration limits optical measurement techniques and resort to physical sampling is necessary.

A high-pressure combustion system designed to provide stable continuous combustion of a liquid spray under reproducible conditions, at pressures approaching those of the diesel cycle, is described. The system provides sufficient access and time for samples to be taken for analysis from the exhaust and selected locations inside the flame. Measurements from this system provide data for comparison with available mathematical models. A relatively rapid, efficient spray combustion model has also been developed, to predict the effect of pressure and input mixture strength on soot

* Corresponding author.
E-mail addresses: r.j.crookes@qmul.ac.uk (R.J. Crookes), gsivali2@ford.com (G. Sivalingam), man@dmu.ac.uk (M.A.A. Nazha), hobina@dmu.ac.uk (H. Rajakaruna).

1290-0729/03/$ – see front matter
doi:10.1016/S1290-0729(03)00029-2

particulate emissions from the experimental system at gauge pressures up to 2 MPa.

2. Experimental

The high-pressure combustion installation (Fig. 1), is focused on a specially developed combustion chamber, shown in Fig. 2, which has evolved from earlier, lower pressure variants [1]. The chamber, designed for a working pressure of up to 10 MPa, is constructed of interlocking and inter-changeable stainless-steel units with a variable-area exhaust (nozzle-plunger) system (Fig. 2) for pressure regulation. When fully assembled the overall length is 0.8 m with diameter 0.15 m.

Air is supplied from a three-stage compressor at 6.5 MPa to a high-pressure receiver through a condensate removal and drier arrangement. The fluctuation-damped, pressure-regulated air stream passes through a flow straightener to ensure plug-flow conditions along the chamber. A gravimetric balance with a digital read-out and a digital flow meter monitor the fuel flow rate to a standard multi-cylinder diesel fuel pump. All outlets of the pump are connected to a high-pressure accumulator to provide a low-fluctuation common-rail fuel supply to a single injector. The injector nozzle has a throat diameter of 0.2 mm and a length/diameter ratio of 2. A fully atomised spray at an injection pressure of 24 MPa gives a diesel fuel mass flow rate of 3.4 $g{\cdot}s^{-1}$ in a single continuous spray along the chamber axis in the same direction as the air-flow. This is the lowest sustainable (blockage-free) flow rate though other flow geometries are possible, including swirling air flow and radial fuel injection. The input equivalence ratio can be varied from about 0.7 to 1.3 by regulation of the air flow for constant fuel supply rate. High-pressure nitrogen gas cuts off the fuel supply to the injector before and after each test to prevent leakage into the chamber at lower pressures. The fuel used was Shell Gas Oil with composition (percentage by mass): *C* (85.44), *H* (12.49), and *S* (0.43). The spray is ignited initially by means of a gas-turbine igniter after which continued combustion is self-sustaining.

Two 12 mm diameter water-cooled, stainless-steel probes have been used: an axial probe located inside the moving plunger of the exhaust nozzle-plunger system, and a radial probe through a sampling port in the sampling section, which is relocateable along the chamber. Soot is collected on fibre-glass filter papers in one of two parallel sealed units, after stable conditions have been established. The concentration of soot in the sampled gases is determined from the mass collected in a recorded time at the steady conditions, together with the metered flow rate of the sample. Measurements are normalised[1] to conditions of standard temperature and pressure or, where appropriate, given at local chamber conditions. Small quantities of soot have also been collected on special grids for examination in

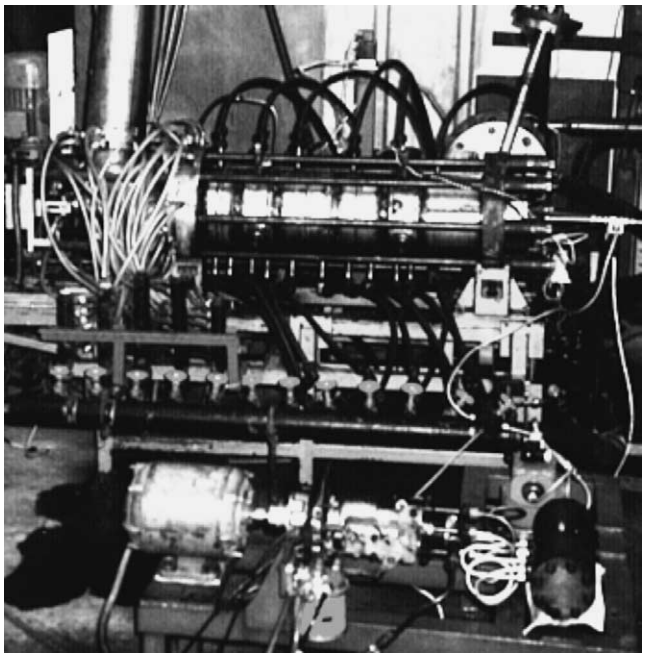

Fig. 1. High-pressure combustion chamber and fuel supply system.

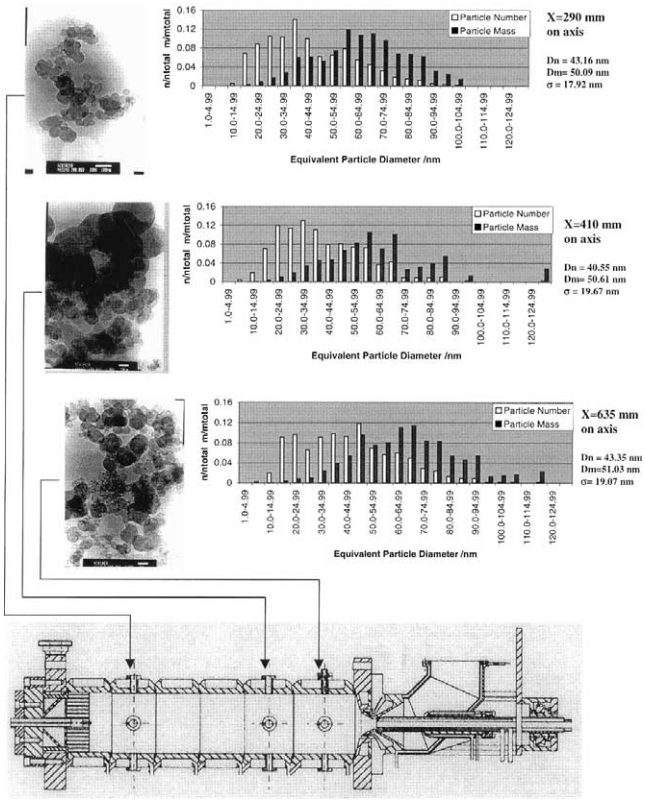

Fig. 2. Soot particle agglomerate size distribution in confined spray flame at different chamber axis locations at 2.1 MPa and stoichiometric input equivalence ratio.

[1] 'Normalised' is used here to indicate that measurements of concentration have been presented for a common standard condition of 101.3 kPa and 288 K and not non-dimensionalised.

a transmitting electron microscope fitted with a CCD camera able to produce images at 500 000 times magnification. The gas sample is passed either through heated or chilled lines, as appropriate, to the standard, regulated emissions analysing instrumentation. Tests have been conducted at combustion pressures between 0.5 and 3 MPa. Results of tests with exhaust gas sampling and in-chamber measurements up to 1.6 MPa have been reported elsewhere [2–4].

3. Predictive model

The computer model used to obtain the predicted results can be applied, with wide parametric variation, to provide rapid feedback [3,5]. In the model it is assumed that the system is a continuous liquid-fuel spray (axi-symmetrical with circular cross-section) burning within a co-flowing, uniform air stream inside a cylindrical combustion chamber under steady conditions. The boundary conditions are the same as the experimental values for pressure, temperature and air and fuel flow rates. A selected Sauter-mean-diameter droplet value and empirically determined droplet velocity are used, based on the experimental injector specification. The properties of gas oil, where available, are used. The model is of the *Locally Homogeneous Flow* (LHF) Type, where the liquid phase is taken into account via a droplet evaporation sub-model, which runs in parallel with the gas-phase Navier–Stokes solver. The novelty of the model is that, it accounts for the changes in the bulk gas-phase (due to liquid fuel evaporation) via an effective property approach, where the property changes resulting from liquid evaporation are allowed to propagate according to the k–ε turbulence model. A comprehensive description of the model and its applicability ranges are given elsewhere [5].

To allow for liquid heating during the evaporation process, the droplet sub-model contained in the code is of a transient heating, spatially unsteady type [6]. The use of the LHF approach for modelling this type of spray is more suitable than the more rigorous *discrete-droplet* formulation due to the high-density gradients encountered in the near injector regions [7,8]. Combustion is considered as a post-processed event, in a *mixed-is-burnt* quasi-adiabatic approach in which, to limit complexity and execution time, the effect of combustion on mixing is neglected and heat transfer is treated indirectly by empirical adjustment of the input enthalpy.

The combustion product-species mole fractions, arrived at by minimising the total Gibbs function for each finite-volume cell, are used in the soot formation and oxidation kinetics sub-models, [9,10]. The soot formation model employed involves semi-empirical kinetic equations including functions of mixture fraction and temperature. In this, Narasimhan [9] arrived at a single first order equation which combined the rates of nucleation and surface growth. There are, of course, many other soot formation models in the literature and two more recent formulations [11,12] have been compared elsewhere [3,4] by the authors at gauge pressures of 1.0 and 1.5 MPa and at 2.0 MPa [13] with the modified model of Narasimhan. This shows it (as is discussed later) to be satisfactory for incorporating into the present model for spray combustion.

4. Results

4.1. Experimental measurements

Fig. 2 shows a sequence of soot-particle agglomerates, sampled from within the combustion chamber at a pressure of 2.1 MPa and stoichiometric input conditions for different axial locations at increasing distances from the injector. Measured primary particle-size distributions for these samples, based on several hundred particles are presented, relative to chamber location. Distributions and mean values of diameter are given in relation to both particle number and mass in the samples. A standard deviation, σ, on the former basis, indicates the spread of diameters.

Fig. 3 illustrates the measured number-mean primary-particle size in agglomerates sampled at axial and radial positions (at a cross-section 0.41 m from the injector) in the chamber, again at the stoichiometric condition and 2.1 MPa. Corresponding variations of experimentally derived soot volume fraction[2] and primary-particle number density are also shown in relation to the sample position in the combustion chamber. While the soot volume fraction and number density decline down the chamber the mean particle diameters seem to remain relatively constant. The measured magnitude of all three parameters decrease slightly radially from the axial value. Broadly, similar trends in number-mean particle diameter at lean and rich conditions and other pressures are shown in Fig. 4. The ranges of variables in experimental tests necessary to produce the comparisons in Figs. 3 and 4 are listed in Table 1 [13].

Two examples of particulate samples collected under non-stoichiometric input conditions at 2.1 MPa are shown in Fig. 5. The first is a highly magnified primary particle, sampled at mid-chamber, axial position with rich input conditions showing a turbostratic structure. The second at mid-chamber, off-axis, under lean input conditions, shows part of an agglomerate with particles exhibiting a wider crystallite spacing, possibly resulting from internal oxidation.

4.2. Computer model predictions

Fig. 6 shows the predicted contours of local vapour-phase equivalence ratio and combustion temperature throughout the combustion chamber for a stoichiometric input air-fuel ratio and a pressure of 2.1 MPa with diesel fuel. The spray appears to remain rich, on the axis, for well over half the chamber length with the highest temperature shown to be

[2] Soot volume fraction is computed from measured soot concentration of local conditions, assuming a value of 2×10^3 kg·m^{-3} for the soot density.

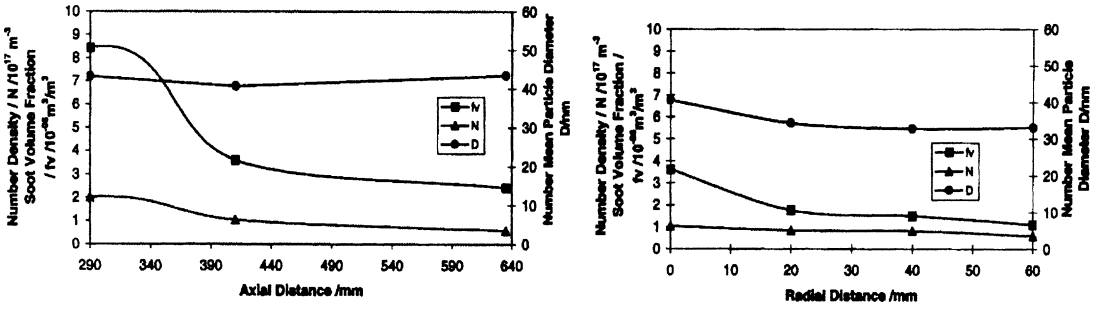

Fig. 3. Measured number-mean particle diameter, primary particle number density and soot volume fraction in agglomerate samples from different axial and radial locations inside combustion chamber at 2.1 MPa and stoichiometric input equivalence ratio.

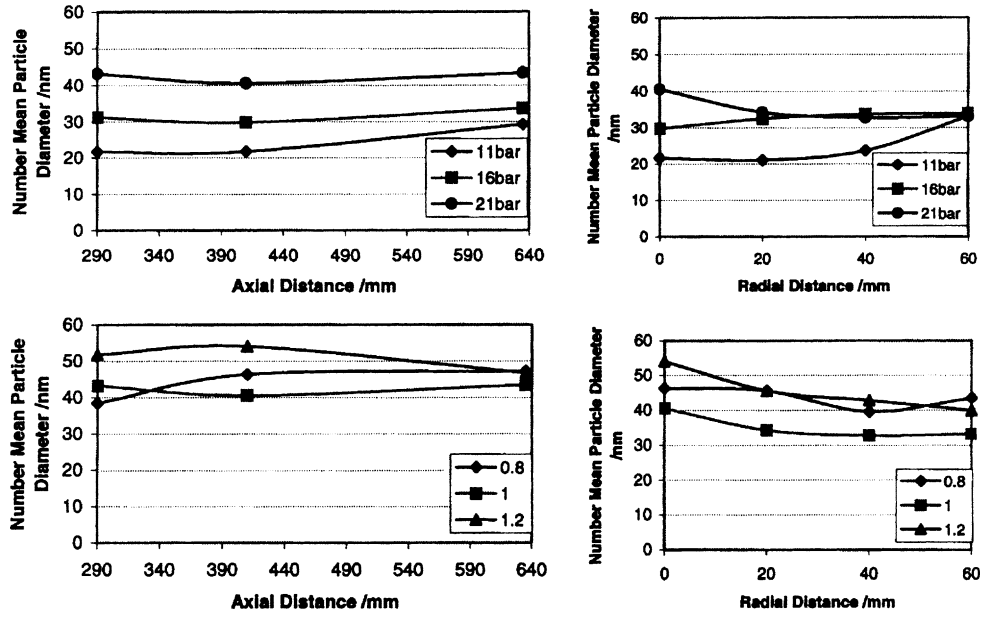

Fig. 4. Measured number-mean particle diameter in agglomerate samples from different axial and radial locations inside combustion chamber at different chamber pressures and input equivalence ratios.

Table 1
Range of experimental tests

Controlled variable	Pressure [MPa]	Equivalence ratio	Sampling location	
			Axial [m]	Radial [mm]
Range	1.1; 1.6; 2.1	0.8; 1.0; 1.2	0.29; 0.41; 0.65	20; 40; 60
Measured parameter	Soot conc [g·m^{-3}]	Particle size		Standard deviation
	(volume fraction)	distribution [nm]	mean dia [nm]	[nm]
Range	0–90 (0–45 × 10^{-6})	10–120	20–60	10–20

just outside the stoichiometric contour, off-centre. Fig. 7 illustrates the effect of changing the input equivalence ratio on the predicted soot distribution at 2.1 MPa. At the rich condition, soot concentration builds up and then reduces along the axis though the highest soot concentration is predicted in an annulus around the axis. Burn-out is much faster at the lean condition. The effect of changing the chamber pressure from 1.6 to 2.1 MPa on the predicted soot distribution at the stoichiometric equivalence ratio is illustrated in Fig. 8. While the patterns are alike and also similar (though less intense) to the rich condition in Fig. 7, the concentration (at local conditions) is increased at the higher pressure and peak values are more focussed in the annular region around the axis.

4.3. Comparison between measurement and prediction

In Fig. 9, a comparison is made between experimental data at 2.1 MPa for input equivalence ratios of 0.8, 1.0 and

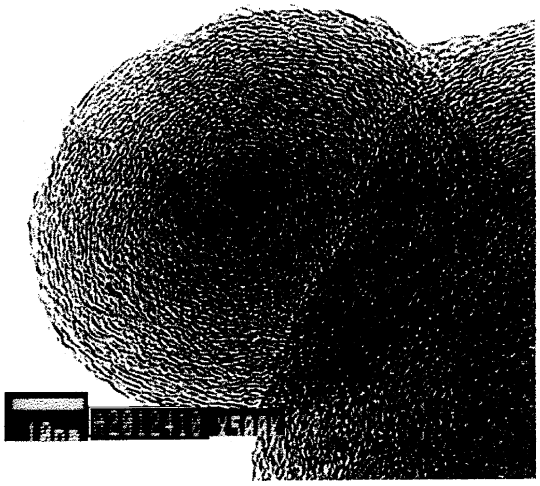

Single primary particle sampled at 41 cm axis, 20 bar and Φ = 1.2

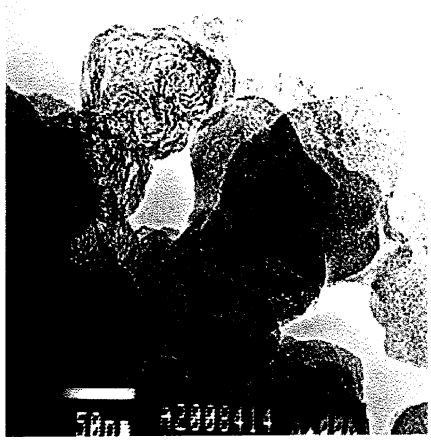

Internally oxdised particles sampled at 41 cm - 4 cm off radial, 20 bar and Φ = 0.8

Fig. 5. Primary particle (rich conditions) and agglomerate (lean conditions) showing crystallite structure at 2.1 MPa.

1.2 with computed axial values of local vapour-phase equivalence ratio and soot concentration normalised to standard conditions of temperature and pressure. The mixture is, in all cases, rich initially on the axis of the spray, subsequently falling to the input value at the exhaust. There is experimental evidence in some cases, of a marginally leaner mid-chamber value, which is commented upon in the next section. The predicted variation of vapour-phase equivalence ratio is in favourable agreement with experimental data. The effects of both pressure and input equivalence ratio on local soot concentration shown in Figs. 9 and 10 are predicted to raise the peak value. When normalised to standard conditions, for comparison with the experimental measurements the curves in Fig. 10 fall closer together at the two pressures. There is qualitative agreement with experimental data at both pressures.

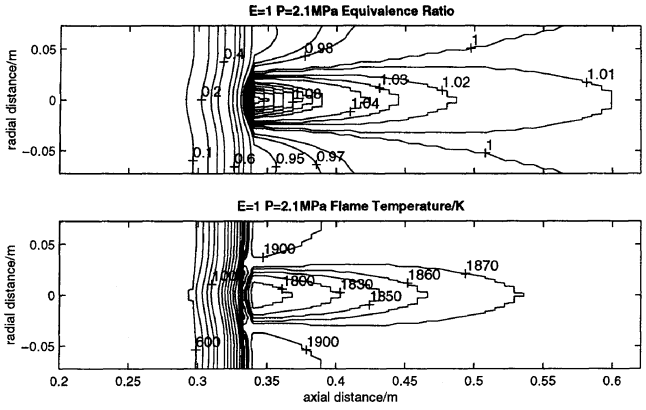

Fig. 6. Computed iso-contours inside combustion chamber of local vapour-phase equivalence ratio and temperature at 2.1 MPa and stoichiometric input equivalence ratio.

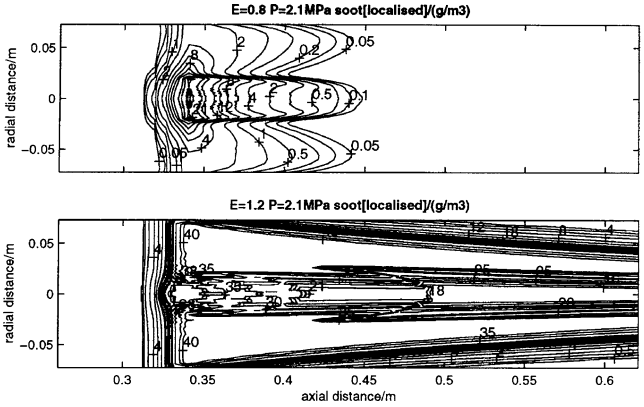

Fig. 7. Computed iso-contours inside combustion chamber of local soot concentration at 2.1 MPa and input equivalence ratios of 0.8 and 1.2.

5. Discussion

The effects of input mixture ratio and chamber pressure are qualitatively predicted and illustrated, at the conditions of the experimental tests (Figs. 7–10) using the current model. The local conditions early in the spray, on the axis, are always rich relative to the input values and subsequently reach these values further along the spray. Conditions favouring soot formation but not oxidation appear to prevail in the rich input spray-flame and soot concentrations are predicted to remain relatively high towards the end of the chamber. At the lean input condition the predicted stoichiometric mixture contour rapidly closes on the spray axis and lean, high temperature conditions result in near total soot burn-out and low net soot concentrations. Burn-out is also predicted to be well advanced at stoichiometric conditions at the end of the chamber. In practice, experimental measurements show chamber exit values to be relatively low at all the input conditions. This burn-out might account for the ultimate small rise in the measured local equivalence ratio at the end of the chamber to the value of the overall input condition. At this location, measured values at 1.6 MPa [4] and particularly at 1.1 MPa [3] were higher showing a lesser de-

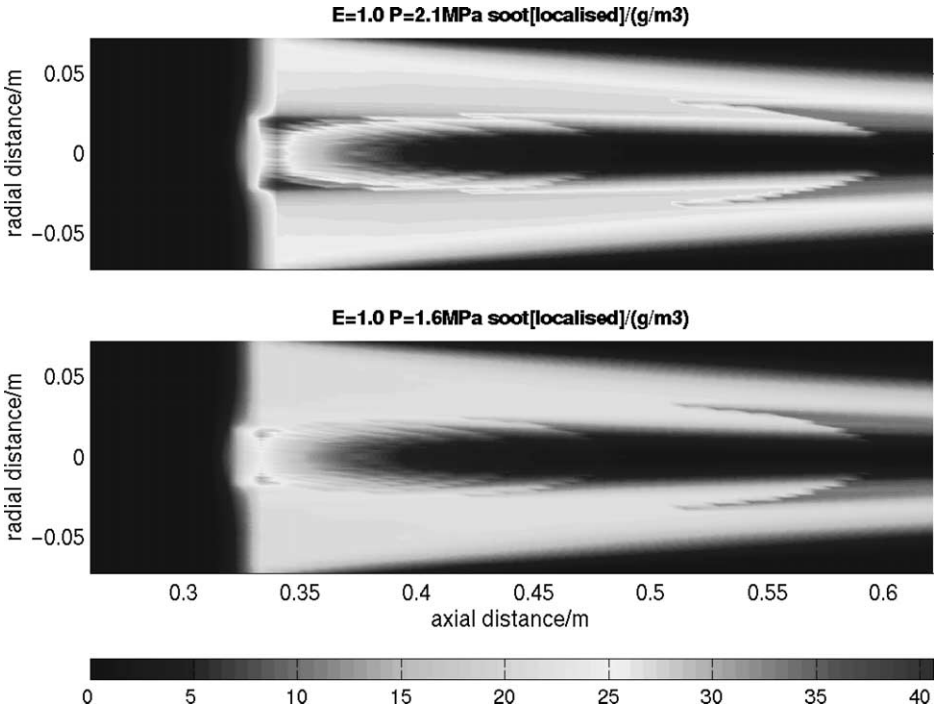

Fig. 8. Map of computed local soot concentration distribution inside combustion chamber at 1.6 and 2.1 MPa with stoichiometric input equivalence ratio.

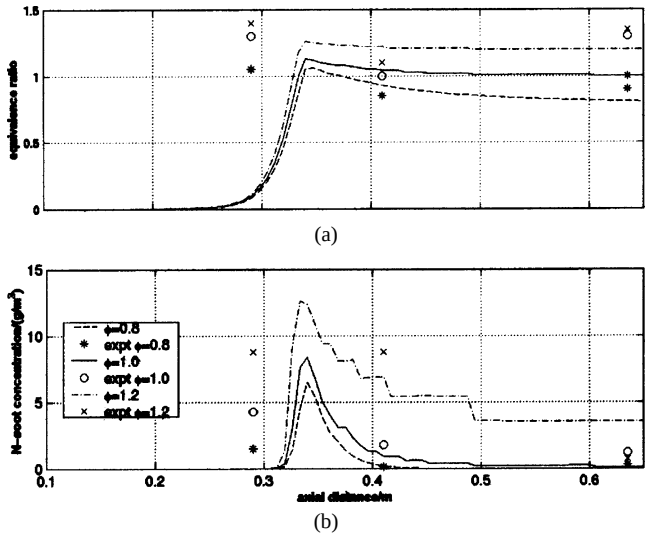

Fig. 9. Comparison of experimental data at 2.1 MPa and input equivalence ratio of 0.8, 1.0 and 1.2 with computed axial values of local vapour-phase equivalence ratio and standardised soot concentration.

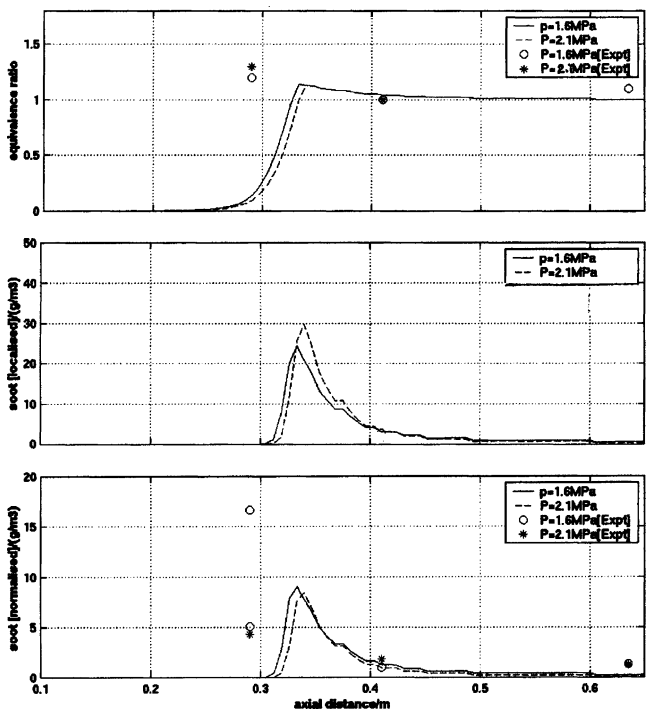

Fig. 10. Effect of chamber pressure on axial values of local vapour-phase equivalence ratio and local and standardised soot concentration at stoichiometric input equivalence ratio.

gree of burn up. This follows logically from consideration of relative flame length and residence time at the different pressures.

Soot concentration measurements at the position of the maximum magnitude in the tests—in the annulus at 20 mm radius, 0.41 m from the injector—showed an increasing focus in this annulus with increasing pressure. For rich input conditions, at 2.1 MPa, maximum measured soot volume fractions (or concentration at local conditions) were 50% higher than at 1.6 MPa [13,14] and as much as six times higher than at 1.1 MPa. For the rich input conditions, values were more than an order of magnitude higher than for the stoichiometric condition. This is consistent with the soot concentration contours in Fig. 7 where the highest value contour also passes through a radial displacement of 20 mm at

mid-chamber length. At the lean input condition, the values were several times lower. Experiments on spray [15–17] and vapourised hydrocarbon flames [18,19], mainly at pressures below 1MPa demonstrated the influence of pressure and input mixture composition, with the pressure dependence having an index higher than unity, becoming linear as pressure increased [19,20]. This was attributed largely to fuel spray preparation in the case of a kerosene spray [16] at pressures up to 1.2 MPa, though unlike in the present work, the spray atomization was air-assisted by part of the combustion air. Present tests indicate a stronger dependence.

In general, predictions indicate lower axial peak values and steeper decay profiles of soot concentration as input conditions become leaner. At the different pressures, the predictions (Fig. 10) produce normalised axial profiles with similar peak height and length showing the results to scale with pressure as in [16]. A comparison of the predicted net soot concentration distribution along the chamber axis using the soot formation models of Moss et al. [11], Nishida and Hiroyasu [12] and Narasimhan [9], has been made by the authors. For each pressure and input mixture ratio the cumulative soot formation and oxidation were computed using a modified version of the in-house spray combustion model [3,4] with the three soot models with the same oxidation mechanism [10]. In all cases, the effect of mixture strength and pressure on the net concentration were similarly and qualitatively predicted though there were quantitative differences and the model of Moss et al. was consistently highest [13]. For the range of experimental data available, the models of Narasimhan and Nishida and Hiroyasu were relatively close, whereas that of Moss et al. varied from closest [3] to farthest [4] as pressure increased. On balance, the predictions using the modified model of Narasimhan were judged not to be significantly improved upon by use of the tested alternative models [13]. The predicted peak values of net concentration are not exactly located by the limited experimental data available and the true maximum values, which are predicted to be off-centre (Fig. 8), of course are not represented in axial diagrams. This is to be addressed by further experimental tests with more, closely-spaced measurements in the expected region of peak soot concentration identified by the predictions.

The particle agglomerates in Fig. 2 have number-mean primary particle diameters in the range 20–50 nm (Fig. 3). This is also true for most conditions [3,4] and locations examined (Fig. 4); such a size consistency follows if nucleation is the dominant formation mechanism at elevated pressures [20,21]. The sizes are in line with those of diesel engine exhaust particles, while the primary-particle size distributions (within an agglomerate) cover a range from 10 to over 100 nm. Mean values were observed to be higher at the higher pressure and richer conditions. These are higher than the values found by Fang et al. [22] in a swirl-stabilised spray burner under lean overall conditions at atmospheric pressure. That the mean value increases very slightly between mid-chamber and the exhaust is in agreement with the findings of Fang et al. They attributed an increase in mean particle size over this span of chamber length-to-radius ratio to a particle growth region. In the present tests, however, this region is one of predominant oxidation and the probable mechanism is one of a self-sustaining size distribution with a net reduction in concentration. This results from a complete consumption of the smaller particles and gradual size reduction of the largest.

The high magnification electron microscopy reveals a regular pattern of crystallite spacing in Fig. 5 of the order of 0.38 nm, a value similar to that found in graphite [23]. There is some evidence of inner nuclear particles and surface layers adjoining primary particles. The spacing in some of the agglomerate particles has been found to be as high as 0.62 nm which could result from internal oxidative reaction under certain conditions [24]. This observation has been associated with carbon black oxidation rather than for diesel particulates. Penetrative as opposed to ablative oxidation would result in different agglomerate morphological histories and mean particle diameters and this is the subject of further examination by the authors and others [13,25].

6. Conclusions

Experimental measurements of steady-state values of local vapour-phase equivalence ratio and soot concentration, at locations inside a high-pressure combustion chamber are presented. Results are for a continuous diesel fuel spray flame, at input equivalence ratios from 0.8 to 1.2 and combustion pressures up to 2.1 MPa. An integrated, two-dimensional (locally-homogeneous flow) computer programme, capable of describing the behaviour of a steady, confined burning liquid-hydrocarbon fuel spray at pressures up to 2.1 MPa and air-fuel ratios from lean to rich has been used to illustrate property variation in the spray.

(1) Measured and predicted soot concentration rose sharply to a peak value and subsequently decayed along the axis of the spray.
(2) Increasing peak soot concentration was measured and predicted at higher pressure (at local conditions) and higher input equivalence ratio. Off-axis maximum values were measured and predicted in an annulus around the position of the axial peak.
(3) Predictions were shown to be in general qualitative agreement with experimental data.
(4) Measured number-mean primary-particle diameters fall in the range 20–50 nm while wide primary-particle size distributions (approx. 10–100 nm) were found in agglomerates at all locations and conditions. Mean diameters increased with increase in pressure and equivalence ratio.
(5) High magnification transmitting electron micrographs of soot particles and agglomerates show graphite-like crystallite spacing 0.38 nm with evidence of enlarged values up to 0.62 nm possibly due to oxidation.

Acknowledgements

The authors wish to acknowledge the financial support for the programme from EPSRC, the contribution of Dr F. Kiannejad in obtaining the experimental burner data and the provision by Queen Mary and Westfield College and DeMontfort University respectively of the experimental and computing facilities.

References

[1] M.A.A. Nazha, R.J. Crookes, SAE 922206, 1992.
[2] R.J. Crookes, F. Kiannejad, M.A.A. Nazha, G. Sivalingam, Measurement of soot-particle emission using a high-pressure continuous spray-combustion facility, Arch. Combust. 16 (1–2) (1996) 23–35.
[3] R.J. Crookes, G. Sivalingam, M.A.A. Nazha, H. Rajakaruna, SAE 1999-01-3488, 1999.
[4] R.J. Crookes, G. Sivalingam, M.A.A. Nazha, H. Rajakaruna, Analysis of soot particulate formation in a confined spray flame at 1.6 MPa, J. Inst. Energy 73 (2000) 134–142.
[5] M.A.A. Nazha, H. Rajakaruna, R.J. Crookes, An effective property, locally homogeneous flow model for liquid fuel spray combustion, Trans. ASME J. Engrg. Gas Turbine Power 122 (2000) 275–279.
[6] H. Rajakaruna, M.A.A. Nazha, Variable finite liquid diffusivity in droplet modelling, in: Internat. Sympos. on Computational Technologies for Fluid/Thermal/Chemical Systems with Industrial Applications, Vol. 377-1, Joint ASME/JSME Pressure Vessels and Piping Conf., 1998.
[7] G.M. Faeth, Progr. Energy Combust. Sci. 9 (1–2) (1983) 1–76.
[8] K.J. Wu, C.C. Su, R.L. Steinberger, D.A. Santavicca, F.V. Bracco, Fluids Engrg., Trans. ASME 105 (4) (1983) 406–413.
[9] K.S. Narasimhan, Kinetics of soot formation in turbulent combustion system with methane, Ph.D. Thesis, University of Sheffield, UK, 1964.
[10] J.P. Appleton, Soot oxidation kinetics at combustion temperature, AGARD-CP-12, 1973.
[11] J.B. Moss, C.D. Stewart, K.J. Young, Combust. Flame 101 (1995) 491–500.
[12] K. Nishida, H. Hiroyasu, SAE 890269, 1989.
[13] G. Sivalingham, Soot particulate formation in a confined diesel fuel spray-flame at elevated pressure, Ph.D. Thesis, University of London, UK, 2001.
[14] R.J. Crookes, G. Sivalingam, M. Nazha, Factors influencing soot particulate formation and oxidation in high-pressure spray combustion, Technologies and Combustion for a Clean Environment Oporto Portugal (2001) 665–671.
[15] M.A.A. Nazha, R.J. Crookes, Proc. Combust. Instit. 20 (1984) 2001–2010.
[16] B.A. Fischer, J.B. Moss, The influence of pressure on soot production and radiation in turbulent kerosene spray flames, Combust. Sci. Techol. 138 (1998) 43–61.
[17] M.S. Janota, R.J. Crookes, S.J. Daie, M.A.A. Nazha, M.N. Sodha, J. Instit. Fuel 402 (1977) 10–13.
[18] W.L. Flower, An investigation of soot formation in axi-symmetric turbulent diffusion flames at elevated pressure, SAND 88-8627, 1988.
[19] K.J. Young, C.D. Stewart, J.B. Moss, Soot formation and turbulence non-premixed Kerosine-air flame burning at elevated pressures: Experimental measurements, Proc. Combust. Instit. 25 (1994) 609–617.
[20] S. Hanisch, H. Jander, Th. Pape, H.Gg. Wagner, Proc. Combust. Instit. 25 (1994) 577–584.
[21] St. Bauerle, Y. Karasevich, St. Slavov, D. Tanke, M. Tappe, Th. Thienel, H.Gg. Wagner, Soot formation at elevated pressures and carbon concentration in hydrocarbon pyrolysis, Proc. Combust. Instit. 25 (1994) 627–634.
[22] T.C. Fang, C.M. Megaridis, W.A. Sowa, G.S. Samuelsen, Combust. Flame 112 (1998) 312–328.
[23] Y. Fujiwara, S. Tosaka, T. Murayama, SAE 901579, 1990.
[24] F.A. Heckman, D.F. Harling, Progressive oxidation of selected particles of carbon black: further evidence for a new microstructural model, in: Mtg. on Rubber Chemistry, American Chemical Society, Florida, USA, 1965.
[25] T. Ishiguro, N. Suzuki, Y. Fujitani, H. Morimoto, Microstructural changes of diesel soot during oxidation, Combust. Flame 85 (1–6) (1991) 1–5.